Super-Hydrophobic Surface Fabricated by the Combination of Layer-by-Layer Electrostatic Self-Assembly Technique and Surface Sol-Gel Method

Yasuhiro Miyauchi, Kouhei Inokuchi, Yuji Sone and Seimei Shiratori

Graduate School of Science and Technology, Keio University,
3-14-1 Hiyoshi, Kouhoku-ku, Yokohama-shi, Kanagawa 223-8522, JAPAN
Fax: +81-45-566-1602, e-mail: yasumiya@appi.keio.ac.jp (Y. Miyauchi); shiratori@appi.keio.ac.jp (S. Shiratori).

Recently, the super-hydrophobic surface, which has water contact angle larger than 150°, has attracted great interests. Both low surface free energy and surface roughness are important parameters for influencing the hydrophobicity of surfaces. In this study, the super-hydrophobic surface was obtained by the combination of the layer-by-layer electrostatic self-assembly (LbL-ESA) technique and the surface sol-gel method. During the LbL-ESA process, the poly(allylamine hydrochloride) (PAH) and poly(acrylic acid) (PAA) were used as polycation and polyanion, respectively. Moreover, titanium tetra-*n*-butoxide was used as metal alkoxide during the surface sol-gel process. By using the combination, we controlled the surface microstructures. The super-hydrophobic surface was obtained by the surface treatment with fluoroalkylsilane (FAS). The fabricated surfaces were evaluated by the contact angle meter, scanning electron microscope (SEM) and atomic force microscope (AFM).
Keywords: super-hydrophobic, layer-by-layer electrostatic self-assembly, surface sol-gel, bearing analysis

1. Introduction

Wettability of the solid surface is the important property for both fundamental and practical aspects, and it strongly depends on both the surface free energy and the surface roughness. When the surface free energy is low, the hydrophobicity is enhanced. Hydrophobicity is attracting great attention to protect from stain and adhesion of snow and so on. Generally, the wettability of the solid surface is commonly evaluated by the contact angle. The water contact angle on the flat surface, which consists of the lowest surface free energy materials (6.7 mJ/m²; closest-hexagonal-packed-CF_3 groups [1]) is about 120° [2].

The research about the wettability of the solid surface has been studied since early times. And, contact angle θ between a flat solid surface and a liquid droplet is given by Young's equation (1) [3].

$$\cos\theta = (\gamma_S - \gamma_{SL}) / \gamma_L \qquad (1)$$

where γ_S, γ_{SL}, and γ_L are the interfacial tensions of solid-vapor, solid-liquid and liquid-vapor interfaces, respectively.

Wenzel suggested that a model describing contact angle θ' of liquid droplets on the rough solid surface [4, 5]. He modified Young's equation to

$$\cos\theta' = r(\gamma_S - \gamma_{SL}) / \gamma_L = r\cos\theta \qquad (2)$$

where r is Wenzel's roughness factor, which is defined as the ratio of the actual area of rough surface to the geometrically projected area. Since r is always larger than 1, surface roughness enhances both hydrophilicity of hydrophilic surface and hydrophobicity of hydrophobic surface.

Cassie and Baxter suggested an equation that the contact angle θ^* on the surface composed of solid and air

[6].

$$\cos\theta^* = \phi_S(\cos\theta + 1) - 1 \qquad (3)$$

where ϕ_S is the solid fraction of the surface.

From eq. (2) and (3), it is important for hydrophobic surface to increase surface roughness and trap air between liquid droplet and solid surface.

Recently, the super-hydrophobic surface, which has water contact angle larger than 150°, has attracted great interests. In natural world, there are plants that exhibit super-hydrophobic properties, such as lotus leaves [7-9]. This phenomenon is caused by a lot of projections on the leaves. And, the projections are coated with hydrophobic wax. To fabricate such surfaces, various methods have been proposed, such as solidification of alkylketene dimmer [10], sol-gel method [11], nanofibers [12,13], crystallization control [14], the phase separation [15], CVD [16], and so on [17-19].

In this study, we report that the fabrication of the super-hydrophobic surface by the combination of layer-by-layer electrostatic self-assembly (LbL-ESA) technique [20], and surface sol-gel method [21].

The LbL-ESA of weak polyelectrolytes, which fabricated monolayer or multilayer films by dipping the substrate successively in each polyelectrolyte solution (polycation or polyanion), can control the thickness and the surface structure by the pH adjustment [19,22-24].

The surface sol-gel method can fabricate ultra-thin inorganic film. Ultra-thin inorganic film is grown on the basis of dehydration or dealcoholation between metal alkoxide and hydroxyl group of the surface. The film was grown by repeating the chemical adsorption of metal alkoxide and hydrolysis of the surface. There are reports about organic/inorganic multilayer by using combination of the LbL-ESA technique and the surface sol-gel method [25,26].

2. Experimental

2.1 Materials

Poly(acrylic acid) (PAA) (M_w = 90,000) was obtained from Polysciences as a 25% aqueous solution. Poly(allylamine hydrochloride) (PAH) (M_w = 70,000) was obtained from Aldrich Chemical. Polyelectrolyte dipping solution of 10^{-2} M (based on the repeat unit molecular weight) was made from 18.2 MΩ pure water. And, the solution's pH was adjusted by NaOH.

Titanium tetra-n-butoxide, monomer (Ti(O-n-Bu)$_4$) was obtained from Kanto Chemical Co, and 2-propanol was obtained from Sigma Aldrich Japan Co, respectively. 0.1 M Ti(O-n-Bu)$_4$ was adjusted by 2-propanol.

Heptadecafluorodecyltrimethoxysilane (FAS), which used for surface hydrophobic treatment, was obtained from Toshiba Silicones Co. FAS was dispersed into hexane, which was obtained from Junsei Chemical Co.

A structural formula of PAA, PAH, Ti(O-n-Bu)$_4$, and FAS is shown in Fig. 1 respectively.

(a) Poly(allylamine hydrochloride)
(PAH)

(b) Poly(acrylic acid)
(PAA)

Bu—O—Ti—O—Bu

Bu: butyl group

(c) Titanium tetra-n-butoxide, monomer (Ti(O-n-Bu)$_4$)

$$(CH_3O)_3 — Si—(CH_2)_2—(CF_2)_7—CF_3$$

(d) Heptadecafluorodecyltrimethoxysilane (FAS)
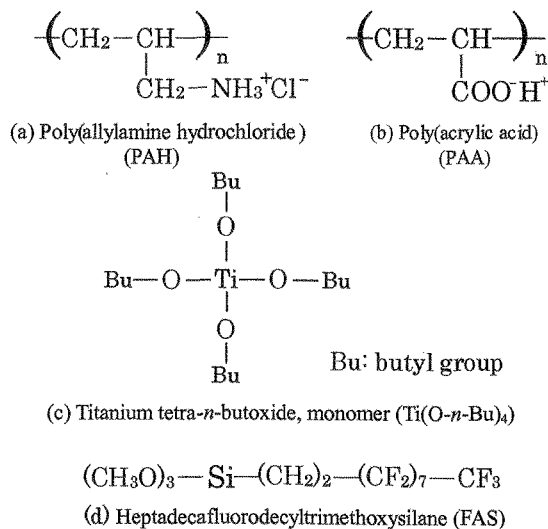
Fig. 1. A structural formula.

2.2 Preparation of LbL film

At first, clean glass substrate was immersed in a polyelectrolyte solution (PAH pH9.5) for 15 min. It immersed in three rinsing baths of water for 2, 1, and 1 min, respectively. Subsequently, immersed in a polyelectrolyte solution (PAA pH6.0) for 15 min, three rinsing baths of water for 2, 1, and 1 min, respectively. These procedures were executed 18 cycles. Thus, LbL film was fabricated.

2.3 Preparation of surface sol-gel film on the LbL film

LBL film was immersed in a 0.1 M Ti(O-n-Bu)$_4$ solution for 3 min. Then, immersed in two rinsing baths of 2-propanol for 3 min respectively. Subsequently, immersed in a water bath (hydrolysis) for 3 min, two rinsing baths of 2-propanol. These procedures were executed from 1 to 8 cycles in globe box (low humidity). Thus, surface sol-gel film on the LbL film was fabricated.

2.4 Hydrophobic treatment process

Surface sol-gel film on the LbL film was immersed in FAS solution for 20 min. And, it is dried at room temperature.

2.5 Surface observation

Surface microstructures of hydrophobic surfaces were observed by an atomic force microscope (AFM, nanoscope III a, Digital Instruments) and scanning electron microscope (SEM, sirion, FEI). Silicon cantilever was used for the tapping mode of the AFM.

2.6 Wettability measurement

Contact angles of water droplets on the hydrophobic surfaces were measured by an optical contact angle meter (CA-DT, Kyowa Interface Science). The contact angles were measured at five different points for each sample.

3. Results and discussions

3.1 Contact angle measurement

Fig. 2 shows photographs of water droplet on the hydrophobic surfaces. It shows that contact angle is increased by both LbL and surface sol-gel. And, Fig. 3 shows a relationship between the number of surface sol-gel cycles on the LbL film and water contact angle. It is found that the water contact angles increase as number of surface sol-gel cycle increase. And, the hydrophobic film changes super-hydrophobic film when the surface sol-gel is 6 cycles. However, water contact angle decrease between 6 and 8 cycles. It is expected that the surface microstructure was changed by surface sol-gel cycle.

(a) Surface sol-gel 6 cycles on the glass substrate (105 °)

(b) Surface sol-gel 6 cycles on the LbL film (150 °)
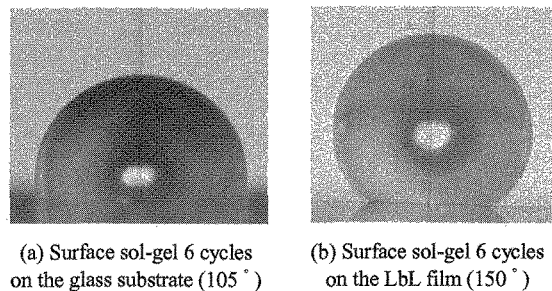
Fig. 2. Photographs of water droplet.
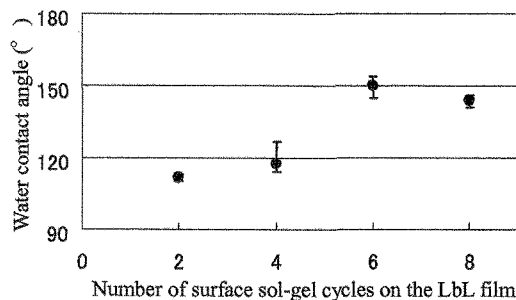
Fig. 3. The relationship between the number of surface sol-gel cycles on the LbL film and water contact angle.

3.2 Observation of the prepared film's surfaces

Fig. 4 shows SEM images of fabricated films. It is found that the surface structure is changed as the cycles of surface sol-gel increase. Enlarged image of the Fig. 4 (d) was shown in Fig. 5. As shown in the figure, numerous nanoparticles were formed on the surface of the texture type structure fabricated by LbL technique. It is considered that the combination of more two order roughness is important for super-hydrophobicity.
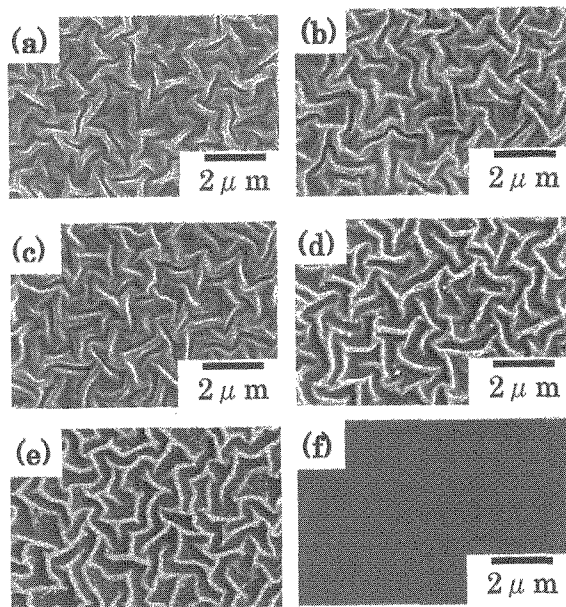
Fig. 4. SEM images of fabricated surface (a) LbL film (b) surface sol-gel 2 cycles (c) 4 cycles (d) 6 cycles (e) 8 cycles on LbL film and (f) 6 cycles on the glass substrate.
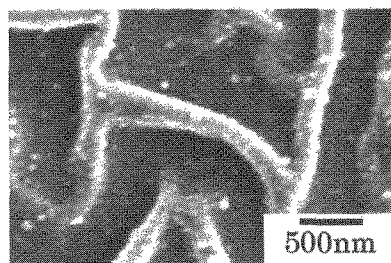
Fig. 5. High magnification of Fig. 4 (d).

According to Fig. 3, water contact angle increase as the cycles of surface sol-gel on the LbL film increase. It is expected that surface roughness is increased by the cycles of surface sol-gel. Therefore, we analyzed these surfaces by AFM (RMS analysis, cross-section analysis and bearing analysis).

3.3 Analysis of the surface structure

In this study, surface roughness (RMS) is calculated by AFM. RMS is the standard deviation of the height values within the given area and it was calculated as

$$RMS = \sqrt{\sum (Z_i - \overline{Z})^2 / N} \qquad (5)$$

where $\overline{Z}$ is the average of the height values within the AFM image, Z_i is the height values, and N is the number of points within the AFM images [18,27]. Fig. 6 shows the results of RMS analysis. It found that RMS values increase as the cycles of surface sol-gel increase. However, in spite of water contact angle was decrease between the cycles of the surface sol-gel, RMS values continued to increase. Bearing analysis was used to explain the reason that RMS values continued to increase.

Bearing analysis reveals the number of a surface lies above or below a given height. This measurement provides additional information beyond standard
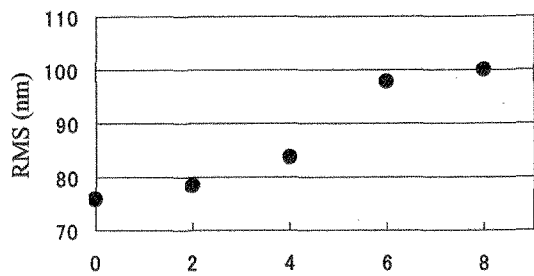
Number of surface sol-gel cycles on the LbL film

Fig. 6. The relationship of between the numbers of the surface sol-gel cycle on the LbL film and RMS.

Fig. 7. Bearing analysis.

(a) The cross-section of the LbL film

(b) The cross-section of surface sol-gel 6 cycles on the LbL film
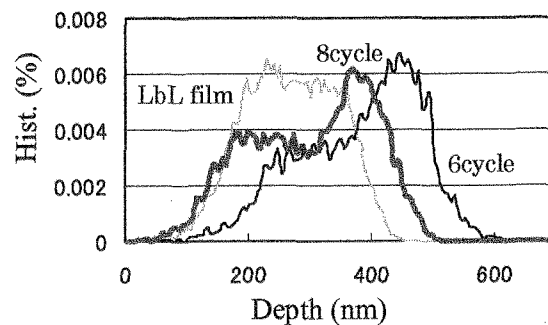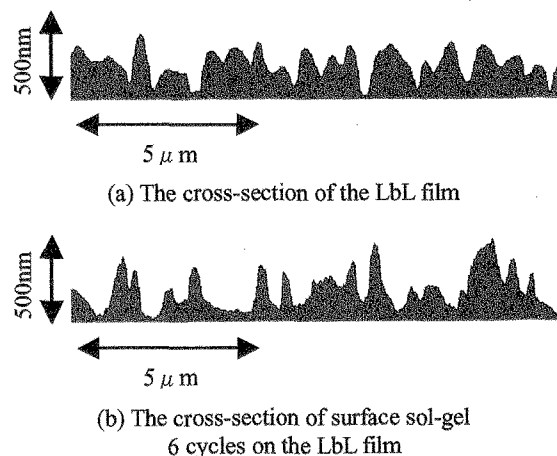
Fig. 8. Cross-section analysis.

roughness measurement [27]. Fig. 7 shows the results of bearing analysis. It is found that the depth distribution was widest when the surface sol-gel 6 cycles on the LbL films, and the depth distribution was narrower somewhat when the surface sol-gel 8 cycles on the LbL films. That is to say, the surface sol-gel 6 cycles had various depth distributions, and accordingly contact angle reached 150°. RMS values were increased for increasing small concavity and convexity between the surface sol-gel 6 and 8 cycles, but the depth distribution was narrower somewhat for the embedding the concavity and convexity when the surface sol-gel 8 cycles on the LbL films. Therefore, the contact angle ware decreased between the surface sol-gel 6 and 8 cycles.

Fig. 8 shows the results of cross-sectional analysis. The structure of LBL film was changed by the surface sol-gel. And, compared Fig. 7 (a) and (b), the structure of Fig. 7

(b) trapped more great amount of air than (a) as expected the existence of the huge water droplet. Since the hydrophobicity is enhanced by the trapped air between the solid surface and liquid droplet, we obtained super-hydrophobic surface. We consider the trapped air is one of the most important factors of hydrophobicity.

Roughness factor was calculated in eq. 2 by the both contact angle of flat surface fabricated by the surface sol-gel 6 cycles on the glass substrate and the contact angle of rough surface fabricated by the surface sol-gel 6 cycles on the LbL films. Roughness factor was calculated as 3.35. Roughness factor calculated by the AFM was 1.33. The difference was caused by the influence of trapped air between the rough surface and water droplet. The equation of Wenzel lost the consideration of trapped air influence. Next, from the equation of Cassie-Baxter (eq. 3), the solid fraction of the rough surface was calculated as 0.18. Hence, the air fraction of the solid surface was 0.82. As a result, the trapped air was one of the most important parameters to influence the surface hydrophobicity.

4. Conclusions

We demonstrated the fabrication of the super-hydrophobic surface using the combination of the LbL-ESA technique and the surface sol-gel method at room temperature. The trapped air was proved to be important parameter for the hydrophobicity of the solid surface. To fabricate such surface, it was considered that the combination of more two orders roughness was important for super-hydrophobicity. This procedure will be applicable to not only for glass substrate but also for flexible substrate, such as PET film.

References

[1] T. Nishino, M. Meguro, K. Nakamae, M. Matsushita, Y. Ueda, *Langmuir*, 15, 4321-4323, (1999)
[2] A. Nakajima, K. Hashimoto, T. Watanabe, *Bull Jpn. Photochem. Assoc.*, 30, 199-206, (1999)
[3] T. Young, *Philos. Trans. Roy. Soc. London*, 95, 65-87 (1805)
[4] R. N. Wenzel, *Ind. Eng. Chem.*, 28, 988-994, (1936)
[5] R. N. Wenzel, *J. Phys. Colloid.Chem.*, 53, 1466-1467, (1949)
[6] A. B. D. Cassie, S. Baxter, *Trans. Faraday Soc.*, 40, 546-551, (1944)
[7] W. Barthlott, C. Neinhuis, *Planta*, 202, 1-8, (1997)
[8] C. Neinhuis, W. Barthlott, *Ann. Bot.*, 79, 667-677, (1997)
[9] L. Feng, S. Li, Y. Li, H. Li, L. Zhang, J. Zhai, Y. Song, B. Liu, L. Jiang, D. Zhu, *Adv. Mater.*, 14, 1857-1860, (2002)
[10] T. Onda, S. Shibuichi, N. Satoh, K. Tsujii, *Langmuir*, 12, 2125-2127, (1996)
[11] K. Tadanaga, K. Kitamuro, J. Morinaga, Y. Kotani, A. Matsuda, T. Minami, *Chem. Lett.*, 864-865, (2000)
[12] L. Feng, Y. Song, J. Zhai, B. Liu, J. Xu, L. Jiang, D. Zhu, *Angew. Chem. Int. Ed.*, 42, 800-802, (2003)
[13] L. Feng, S. Li, H. Li, J. Zhai, Y. Song, L. Jiang, D. Zhu, *Angew. Chem. Int. Ed*, 41, 1221-1223, (2002)
[14] H. Y. Erbil, A. L. Demirel, Y. Avci, O. Mert, *Science*, 299, 1377-1380, (2003)
[15] A. Nakajima, K. Abe, K. Hashimoto, T. Watanabe, *Thin Solid Films*, 376, 140-143, (2000)
[16] A. Hozumi, O. Takai, *Thin Solid Films*, 334, 54-59, (1998)
[17] A. Nakajima, *J. Ceram. Soc. Jpn.* 112, 533-540, (2004)
[18] T. Soeno, K. Inokuchi, S. Shiratori, *Trans. Mater. Res. Soc. Jpn.*, 28, 1207-1210, (2003)
[19] K. Inokuchi, S. Shiratori, *Jpn. Soc. Appl. Phys.*, 65, 1074, (2004)
[20] G. Decher, *Science*, 277, 1232-1237, (1997)
[21] I. Ichinose, H. Senzu, T. Kunitake, *Chem. Mater.*, 9, 1296-1298, (1997)
[22] S. S. Shiratori, M. F. Rubner, *Macromolecules*, 33, 4213-4219, (2000)
[23] D. Yoo, S. S. Shiratori, M. F. Rubner, *Macromolecules*, 31, 4309-4318, (1998)
[24] K. Inokuchi, S. Shiratori, *Soc. Poly. Sci. Jpn.*, 53, 2PF038, (2004)
[25] T. Ito, Y. Okayama, S. Shiratori, *Thin Solid Films*, 393, 138-142, (2001)
[26] Y. Maehara, S. Takenaka, K. Shimizu, M. Yoshikawa, S. Shiratori, *Thin Solid Films*, 438, 65-69, (2003)
[27] Nanoscope Command Reference Manual, Digital Instruments, Ch. 13-14, (2001)